Digest Journal of Nanomaterials and Biostructures Vol. 9, No. 4, October - December 2014, p. 1713 - 1727

INVESTIGATION OF PRISTINE AND FUNCTIONALIZED SINGLE-WALLED CARBON NANOHORNS FOR PHOSPHOR APPLICATIONS

D. KUMAR*, KAVITA[a], K. SINGH, V. VERMA[b] , H. S. BHATTI
Department of Physics, Punjabi University, Patiala-147002, Punjab, India
[a]Department of Physics, M M Modi College, Patiala-147001, Punjab, India
[b]Department of Physics, Govt. College, Naya Nangal, Distt Ropar 140126, Punjab, India

Carbon nanohorns represent a largely unexplored carbon allotrope within the family of fullerenes and carbon nanotubes. There are three critical points that differentiate carbon nanohorns (CNHs) from carbon nanotubes (CNTs), namely, i)purity, due to the absence of any metal nanoparticles during production, ii) heterogeneous surface structure, due to highly-strained conical-ends, and, iii) aggregation in spherical superstructures, typically ranging between 50-100 nm. In the present investigation single wall carbon nanohorns have been synthesized by submerged arc method followed by hydroxyl and carboxylic addent functionalization using high speed vibration method to make them water soluble. Crystallographic, topographic and morphological analyses of pristine and water soluble SWCNHs have been studied via powder X-ray diffraction, field emission scanning electron microscope, high resolution transmission electron microscope and atomic force microscope respectively. UV-Vis. absorption, Raman spectroscopy, thermogravemetric analysis, X-ray photo electron spectroscopy and Fourier transform infra-red spectroscopic studies have been carried out for the functionalization confirmation. Optical, quantitative and qualitative analysis of the pristine and functionalized single wall carbon nanohorns (SWCNHs) have been conceded via energy resolved and time resolved photoluminescence and energy dispersive X-ray spectroscopic studies respectively. Spectroscopic studies confirm the formation of good quality pristine and functionalized SWCNHs with hydroxyl and carboxylic group addent Spectroscopic studies confirm the formation of good quality pristine and water soluble SWCNHs. The presented method demonstrated its remarkable potentiality in large-scale production of SWCNHs with good purity. Structural analyses of synthesized and functionalized SWCNHs have been studied using Brunauer-Emmett-Teller Surface area analysis Barrett-Joyner-Halenda pore size and volume analysis Technique.

(Received October 5, 2014; Accepted December 17, 2014)

Keywords: SWCNHs, submerged arc method, Crystallographic, Topographic, Morphological and spectroscopic studies

1. Introduction

Single-walled carbon nanohorn (SWCNH) is the name given by Sumio Iijima and colleagues in 1999 to horn-shaped sheath aggregate of graphene sheets. [1-2] Very similar structures had been observed by Peter et. al,.[3] in 1994. Ever since the discovery of the fullerene, [4] the family of carbon nanostructures has been steadily expanded. Included in this family are single-walled (SWCNTs) and multi-walled carbon nanotubes (MWCNTs), [5] carbon onions and cones and, most recently, SWCNHs. These SWCNHs with about 40–50 nm tubule length and 2–3 nm in diameter are derived from SWCNTs and ended by a five-pentagon conical cap with a cone opening angle of ~20^o.[6-8] Moreover, thousands of SWCNHs associate with each other to form

*Corresponding author: dineshk_2@yahoo.co.in

the ‘dahlia-like' and ‘bud-like’ structured aggregates which have an average diameter of about 80-100 nm. The former consists of tubules and graphene sheets protruding from its surface like petals of a dahlia, while the latter is composed of tubules developing inside the particle itself.[9] Their unique structures with high surface area and micro porosity make SWCNHs a promising material for gas adsorption, biosensing, drug delivery,[10] gas storage[11] and catalyst support for fuel cell [12] Single-walled carbon nanohorns are an example of the family of carbon nanocones SWCNHs can be synthesized with high purity by CO_2 laser ablation [1] and arc discharge without any metal catalyst [13]. The size and purity of the SWCNHs can be changed by varying the parameters such as temperature, pressure, voltage and current. Various methods have been developed to functionalize carbon nanohorns including covalent bonding, π-π stacking, supramolecular assembly and decoration of metal nanoparticles. [14-22]. The present research paper make use of submerged arc method for production of SWCNHs and then utilized high speed vibration method (HSVM) to functionalize these materials with hydroxyl and carboxylic groups to make them water soluble.

2. Experimental Details

2.1 Synthesis of SWCNHs

A dc arc discharge was generated between two graphite electrodes submerged in 2000 cm^3 of liquid nitrogen in a thick glass vessel. The arc discharge was initiated in the liquid nitrogen by touching a 99.99% purity graphite anode (3 mm in diameter) with a graphite cathode (12 mm tip diameter) of similar purity. The arc voltage and current were typically 34 V and 50 A, respectively.. The gap between the electrodes was manually controlled by a screw unit so that they always remain at a separation of approximately 1 mm by continuously translating the anode during the experiment in order to maintain a stable discharge. The arc discharge in liquid nitrogen is turbulent, and dense black smoke is observed near the discharge region. The evaporation rate of liquid nitrogen was about 200 cm^3 min^{-1} and the anode consumption rate was about 375.3 $mgmin^{-1}$. In contrast to the discharge in water, the products from the arc discharge in liquid nitrogen settle exclusively at the bottom of the reaction container.

2.2 Functionalization of SWCNHs with hydroxyl and carboxylic group

10 g of succinic anhydride (100 mmol) fine powder were added to 20 ml of an ice cold solution of 8 % hydrogen peroxide (52 mmol). The mixture was stirred for about 1 hour at 0 °C. The white gel-like solution was filtered through a 5 μm polycarbonate filter. The resulting succinic acid acyl peroxide was washed with cold distilled water, and then dried under vacuum at room temperature for about 24 hours. Approximately 6 g of succinic acid acyl peroxide was obtained. Again 5 mg of this sample was mixed with 100 equiv. (mass ratio) of succinic acid acyl peroxide. The resulting mixture was put in a stainless steel beaker and shaken vigorously for 1.5 hours @1725 rpm which leads to an ultrafine powder. This ultrafine powder was washed with a large amount of acetone and centrifuged to remove any organic residues not associated with the SWCNHs. The supernatant was carefully decanted. This process was repeated three times and the solid was washed with pure water once. In this way hydroxyl and carboxylic group are attached with SWCNHs.

3. Characterization

Crystallography of pristine and functionalized SWCNHs were characterized by powder X-ray diffraction (XRD) (Rigaku Japan, Miniflex 600), Topography of these nanostructures were characterized by field emission scanning electron microscope (FESEM) (SUPRA 55 OX-FORD INSTRUMENTS) & Atomic force microscope (AFM) (Park XE 70), Morphology of synthesized and functionalized SWCNHs was characterized by high resolution transmission electron

microscope (HRTEM) (Hitachi (H-7500)), Fourier Transform Infrared Spectroscopy (FTIR) (Perkin Elmer - Spectrum RX-IFTIR), UV-Vis. absorption spectroscopy (Hitachi-330 spectrophotometer), Micro-Raman spectroscopy was performed on "Renishaw in Via Raman microscope". using Ar^+ laser as an excitation source with 514 nm line, X-ray Photoelectron spectroscopy (XPS) (kratos axis ultra DLD) was performed for detailed quantative and qualitative analysis. Optical characterization were performed using steady state Photoluminescence (PL) spectroscopy (Perkin Elmer LS 55 Fluorescence spectrophotometer), and time resolved fluorescence spectroscopy (Edinburgh FL 920 Fluorescence life time spectrometer) and energy dispersive X ray spectroscopy (EDS) Thermogravometric analysis [TGA-DSC-DTA] (Perkin Elmer STA 6000), surface area and pore size determination using BET-BJH technique (Nova 2000e Quantachrome) was performed

Results and Discussion

The phase identification from the recorded XRD patterns in fig. 1 has been carried out with the help of standard JCPDS data base. Comparison of XRD patterns with JCPDS No. 23-64, P63/mmc have confirmed that diffraction peaks correspond to the hexagonal wurtzite crystal structure having lattice parameters a =5.657 Å c =6.721 Å.

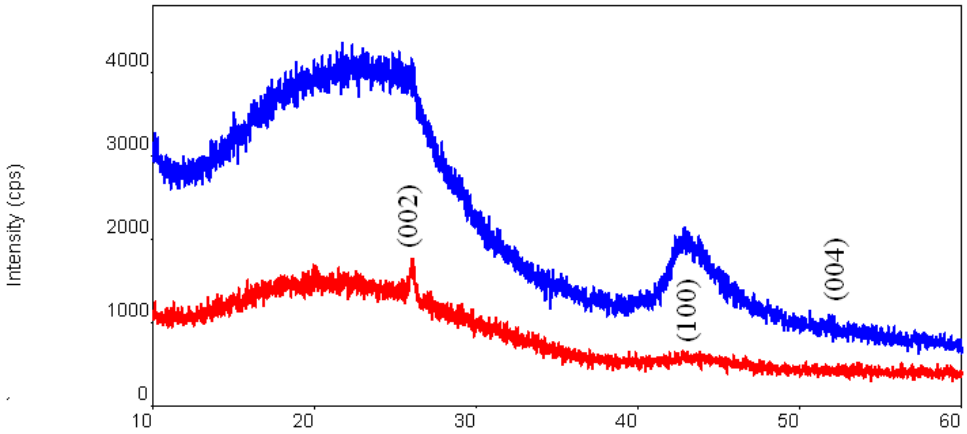

Fig. 1. XRD Pattern of Pristine (Red) and water soluble (Blue) SWCNHs

Average crystallite size can be calculated from the line broadening of the diffractogram peaks using Scherrer formula

$$D = \frac{0.89\lambda}{\beta cos\theta} \quad (1)$$

Where D is the average crystallite size, λ is incident X-ray wavelength, β is the full width half maximum (FWHM) of diffraction peak expressed in radians and θ is peak position in X-ray diffractogram.. Average crystalline size for synthesized SWCNHs is 2.371 nm where as for water soluble SWCNHs it is 1.072nm.

Figures 2 and 3 shows FESEM micrograph recorded for pristine and functionalized SWCNHs. FESEM micrograph in fig. 2 shows agglomerated (dahia) SWCNHs where as fig. 3 FESEM micrograph shows topography of water soluble SWCNHs. Morphology of synthesized SWCNHs derivatives have been investigated by HRTEM. HRTEM micrograph of all the compounds revealed the presence of nanohorns; in all cases the pictures consisted of small round shaped aggregates with diameters of about 80-100 nm in which it was possible to distinguish small conical caps pointing out and the same is visible from micrograph fig. 4. Almost no difference can be noticed between the pristine material and the water soluble nanohorns and the same is revealed

from micrograph shown in fig. 5. Recorded energy dispersive spectra in fig 6 confirm that the carbon content in synthesized SWCNHs is 89.19 wt % along with 10.81 wt % oxygen where as in case of water soluble SWCNHs carbon content is 83.95 wt% along with 16.05 wt% oxygen

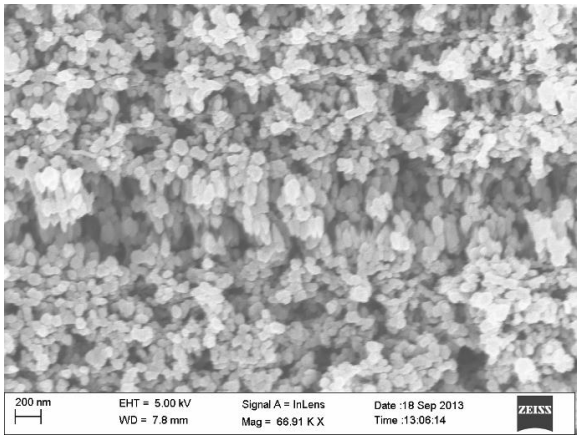

Fig. 2 FESEM micrograph of SWCNHs

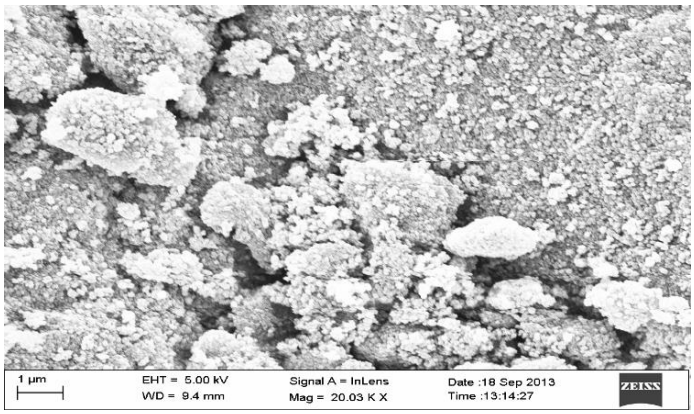

Fig. 3. FESEM micrograph of water soluble SWCNHs

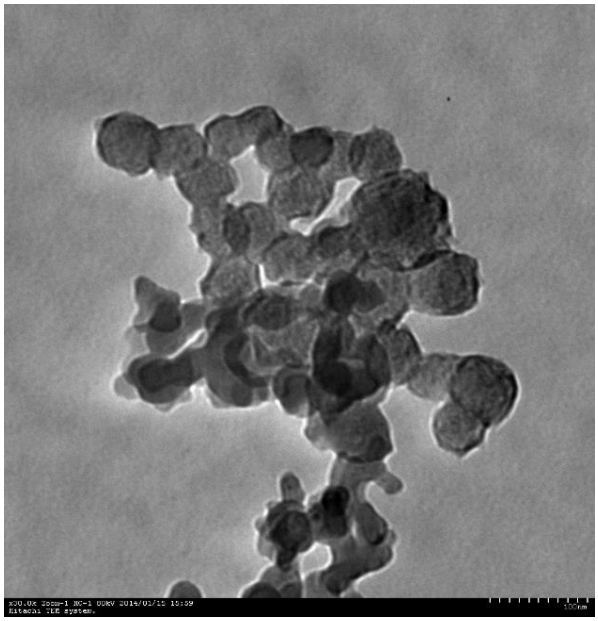

Fig. 4. HRTEM micrograph of SWCNHs

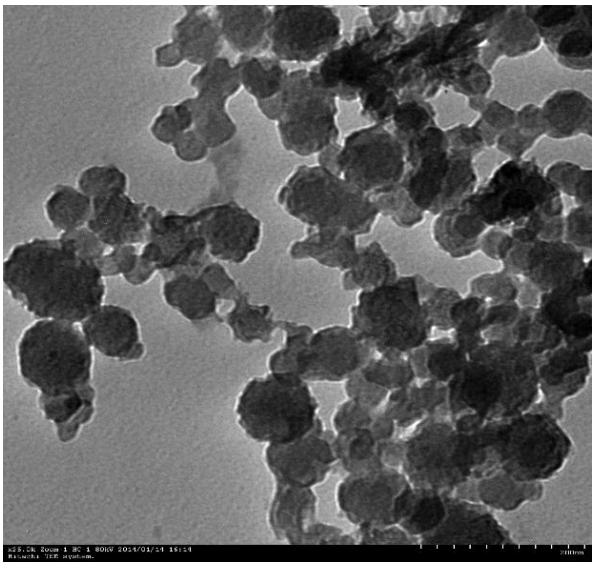

Fig. 5. HRTEM micrograph of water soluble SWCNHs

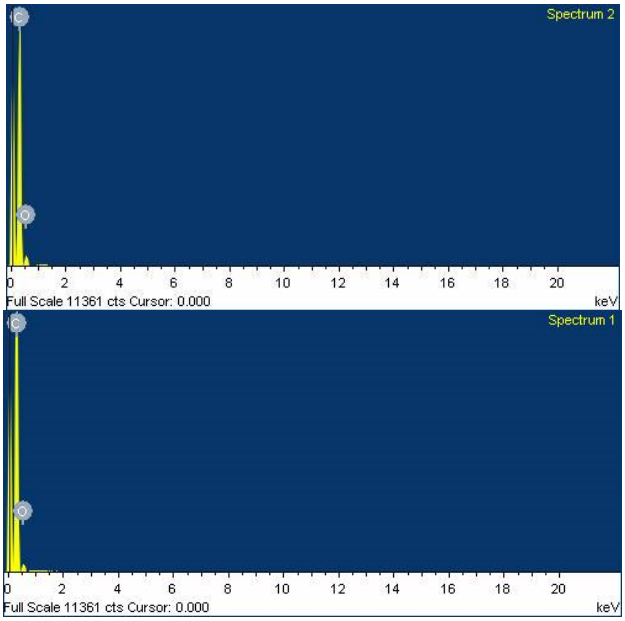

Fig. 6. EDS of SWCNHs and water soluble SWCNHs

Topography and morphology of synthesized nanohorn derivatives have been recorded by AFM as shown in fig. 7. The samples were prepared by doctor blade coating on a mica substrate from a solution/suspension of the material in PVA.

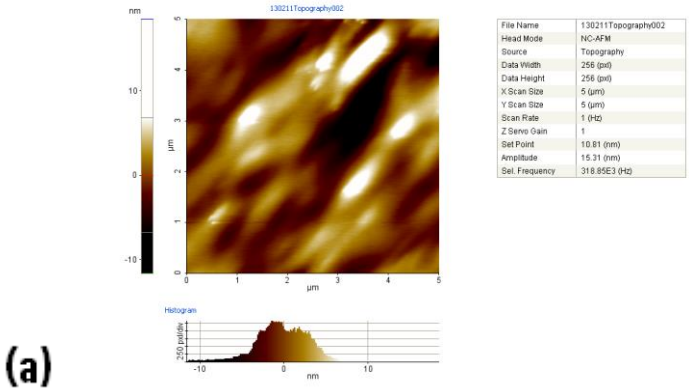

File Name	130211Topography002
Head Mode	NC-AFM
Source	Topography
Data Width	256 (pxl)
Data Height	256 (pxl)
X Scan Size	5 (μm)
Y Scan Size	5 (μm)
Scan Rate	1 (Hz)
Z Servo Gain	1
Set Point	10.81 (nm)
Amplitude	15.31 (nm)
Sel. Frequency	318.85E3 (Hz)

(a)

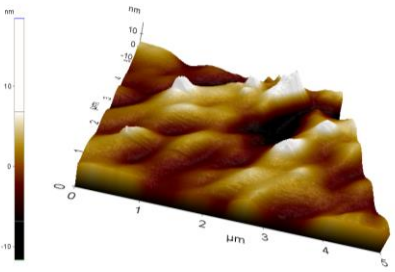

File Name	130211Topography002
Head Mode	NC-AFM
Source	Topography
Data Width	256 (pxl)
Data Height	256 (pxl)
X Scan Size	5 (μm)
Y Scan Size	5 (μm)
Scan Rate	1 (Hz)
Z Servo Gain	1
Set Point	10.81 (nm)
Amplitude	15.31 (nm)
Sel. Frequency	318.85E3 (Hz)

(b)

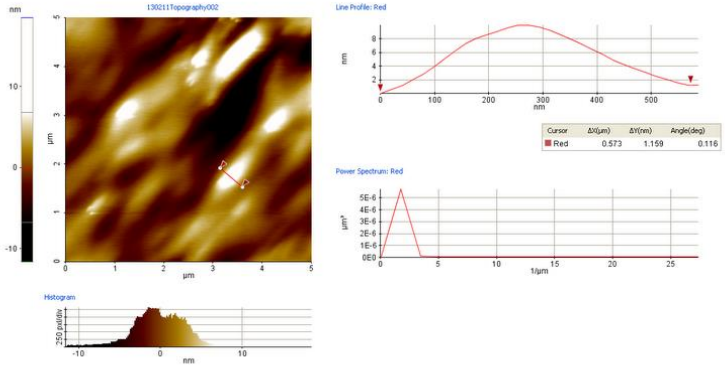

Cursor	Δx(μm)	Δy(nm)	Angle(deg)
Red	0.573	1.159	0.116

(c)

Statistics

Line	Min(nm)	Max(nm)	Mid(nm)	Mean(nm)	Rpv(nm)	Rq(nm)	Ra(nm)	Rz(nm)	Rsk	Rku
Red	0.039	9.955	4.997	5.360	9.916	3.152	2.812	N/A	0.049	1.621

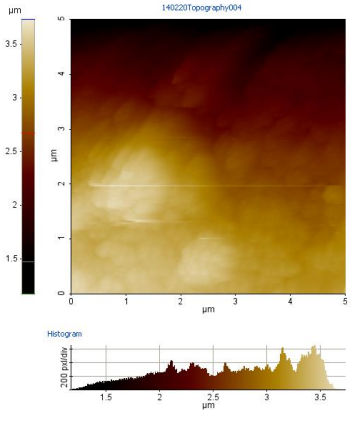

File Name	140220Topography004
Head Mode	MFM
Source	Topography
Data Width	256 (pxl)
Data Height	256 (pxl)
X Scan Size	5 (μm)
Y Scan Size	5 (μm)
Scan Rate	0.5 (Hz)
Z Servo Gain	1
Set Point	8.91 (nm)
Amplitude	12.4 (nm)
Sel. Frequency	83.203E3 (Hz)

(d)

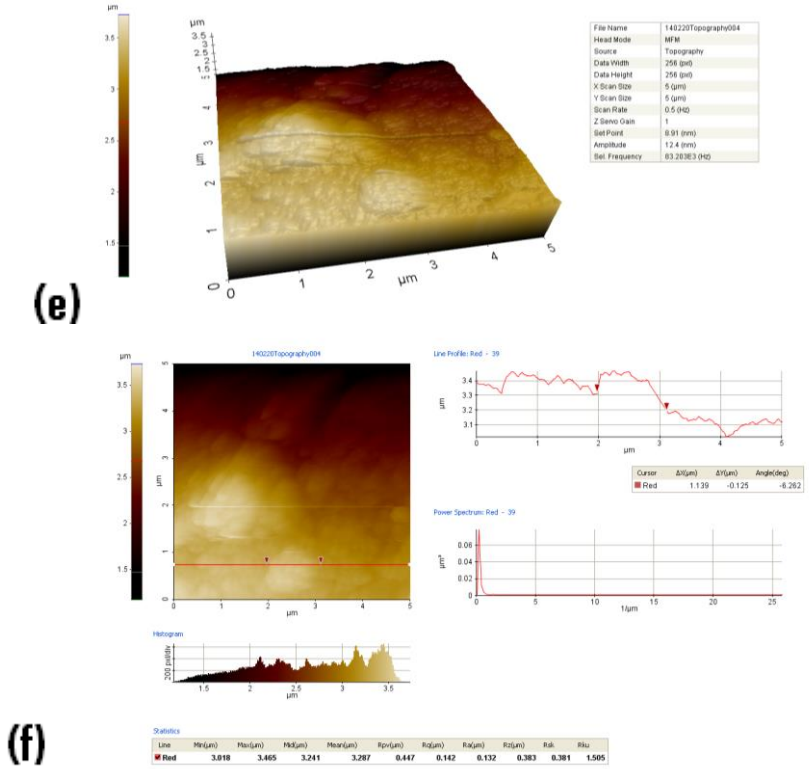

Fig 7. (a-c) AFM of SWCNHs (d-f) water soluble SWCNHs

The images revealed in all cases the coexistence of individual SWCNHs (round shapes of about 60-100 nm diameter) as well as aggregates several hundred nanometers high. Two representative images of SWCNHs fig 7 (a-c) and water soluble SWCNHs fig 7 (d-f) are shown; the use of AFM allow us to see the fine structure of the nanohorns, in fig. 7 (a and b) and only some asperities on the surface have been observed in fig. 7 (d and e).AFM micrograph fig 7(c) and 7 (f) also reveals that surface area after functionalization increases. AFM micrograph reveal that morphological parameters calculated from the AFM micrograph are in proximity with HRTEM recorded.

The Raman spectra of nanohorns in fig. 8 exhibits broad peak at 1593 cm^{-1} ("G-band"), assigned to tangential vibrations in the sp^2-bonded carbon network and another broad peak at 1341 cm^{-1} (''D-band''), attributed to the disruption of the basal plane lattice due to the conical terminated tips of the nanohorns as well as to sp^3 single bonding carbon atoms existing within SWCNHs aggregates.

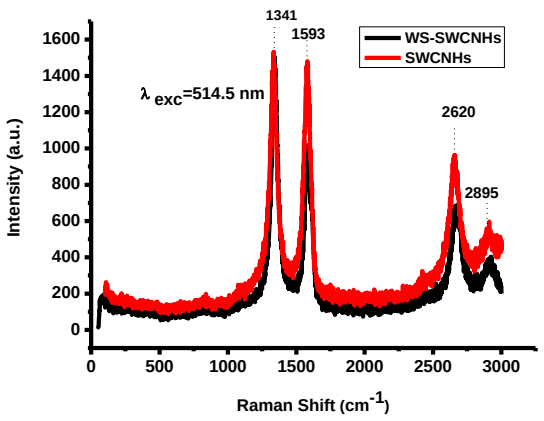

Fig. 8. Raman spectra of SWCNHs and water soluble SWCNHs

The increased intensity around the D-band of water soluble SWCNHs compared with pristine SWCNHs indicates the generation of sp^3-hybridized carbon atoms in the SWCNHs framework.[23-24] The recorded spectra show the G' band (overtone of the D band) at 2620 cm^{-1} and a characteristic band at 2895 $cm^{-1.}$

UV-Vis absorption spectra of water soluble SWCNHs exhibit sharp maxima at 220nm and then decreases monotonically and similar to pristine SWCNHs and the same are revealed from fig. 9.

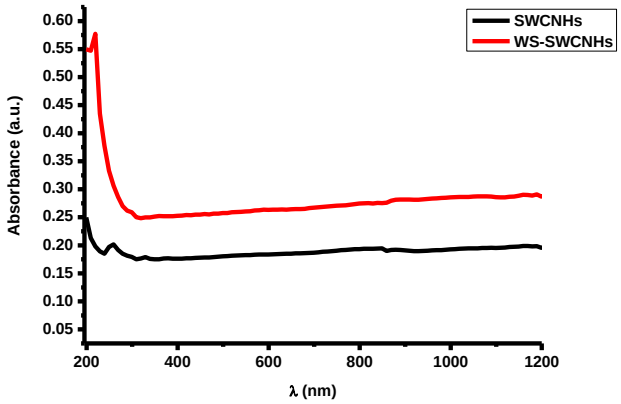

Fig. 9. UV-Vis absorption spectra of SWCNHs and water soluble SWCNHs

FTIR spectra of SWCNHs and water soluble SWCNHs is shown in fig. 10. Peaks at 1061, 1114, 1164cm^{-1} represent C-O stretching. All spectra show characteristic C-C stretching at 1633 cm^{-1}. Peaks at ~2914 cm^{-1} can be related to the symmetric and asymmetric vibrations of C-H group. The peaks at around 3300-3500 cm^{-1} are ascribed to the O-H vibration.

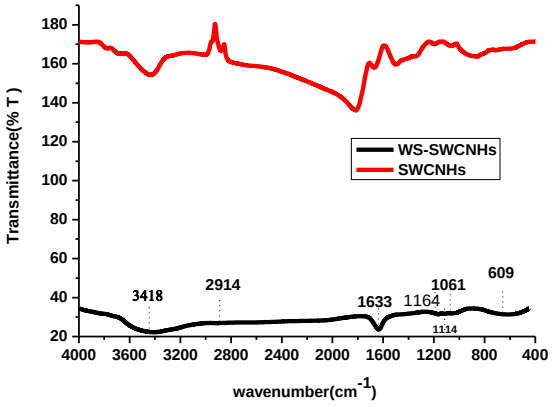

Fig. 10 .FTIR spectra of SWCNHs and water soluble SWCNHs

TGA has been widely used to evaluate the purity of the SWCNHs and this analysis has been performed in air flow. Material combustion below 400^0C is basically due to amorphous carbon From fig. 11 in the derivative curves different phases are well observable: an amorphous phase peak at 400°C, followed by peaks related to SWCNHs, and almost two peaks ascribable to residual graphitic structures for gaint graphitic balls and graphene. Results clearly indicate no metal impurity is present. Purity of water soluble carbon nanohorns have been evaluated in fig. 12. The weight loss up to 80^oC is due to water molecules associated with the surface of SWCNHs followed by removal of hydroxyl and carboxylic groups and then followed by peaks related to SWCNHs.

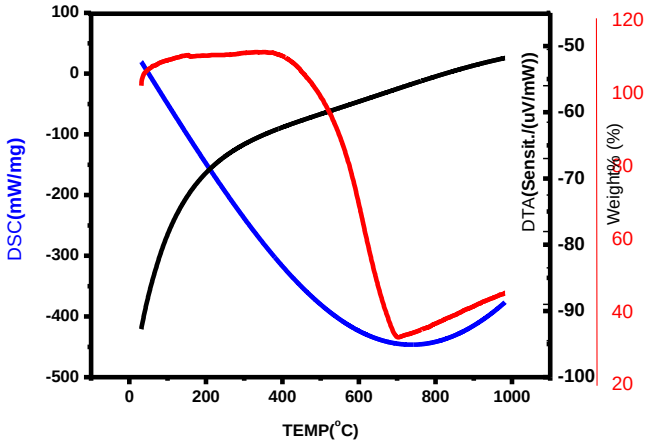

Fig. 11. TGA-DSC-DTA analysis of SWCNHs

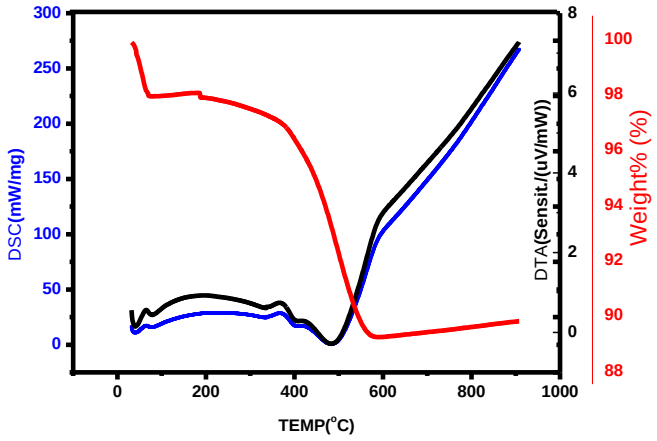

Fig. 12. TGA-DSC-DTA analysis of water soluble SWCNHs

From fig 13 (a) XPS survey results reveal that the O/C atomic ratio of water soluble-SWCNHs (13.5:86.5) dramatically increases relative to that of the pristine SWCNHs (3.3:96.7) and no other impurities were detected. Figs. 13 (b and c) show the high resolution C1s spectra of both SWCNHs and water soluble SWCNHs revealing two types of major carbon peaks corresponding to carbon atoms with different functional groups.

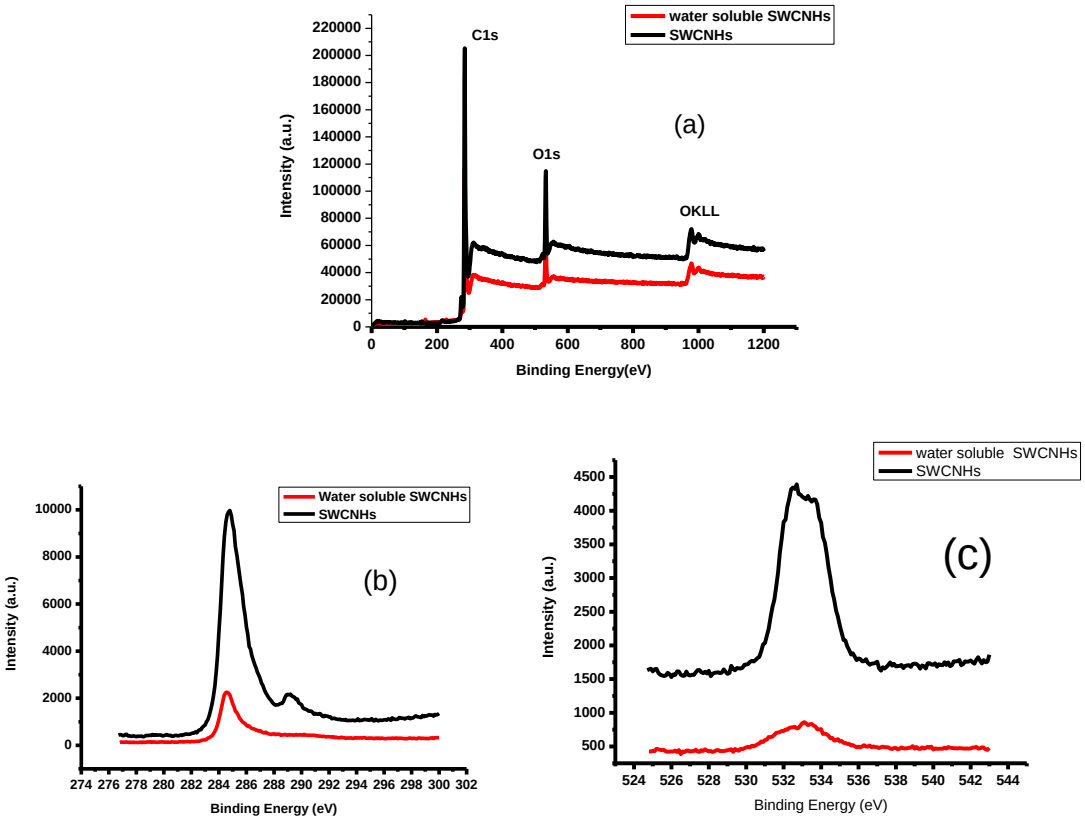

Fig. 13 (a) XPS survey (b) C1s and (c) O1s spectra of SWCNHs and water soluble SWCNHs

Deconvoluted C1s spectrum of SWCNH and water soluble SWCNH shows the main peak at 284.1ev which is attributed to the Sp^2 carbon and the peaks observed for C1s of C-C Sp^3at 285.2ev, C1s of C=O at 288.1ev. All these peaks are suppressed when hydroxyl and carboxylic groups are attached indicating water soluble SWCNH. Deconvoluted O1s XPS spectrum of water soluble SWCNH which is wide and asymmetric, demonstrating that there was more than one chemical state. The presence of lattice oxygen is confirmed from the most intense peak at 530.6ev.Other peaks at 534.2eV and 532.6eV are related to surface hydroxyl groups O–H and single C–O bonds respectively and all these peaks are in stretched state as compared to SWCNH. The additional peak at 533.2eV in suppressed condition appeared in case of water soluble SWCNH confirming surface modification indicates both hydroxyl and carboxylic groups are attached.

Fig 14 reveals the texture property of pristine and water soluble SWCNHs. The surface area and total pore volume as measured by the BET method (calculated by N_2 gas adsorption on the surface of the materials) of water soluble SWCNHs (1014.707 m^2/g) is much higher than that of pristine SWCNHs (125.616 m^2/g).

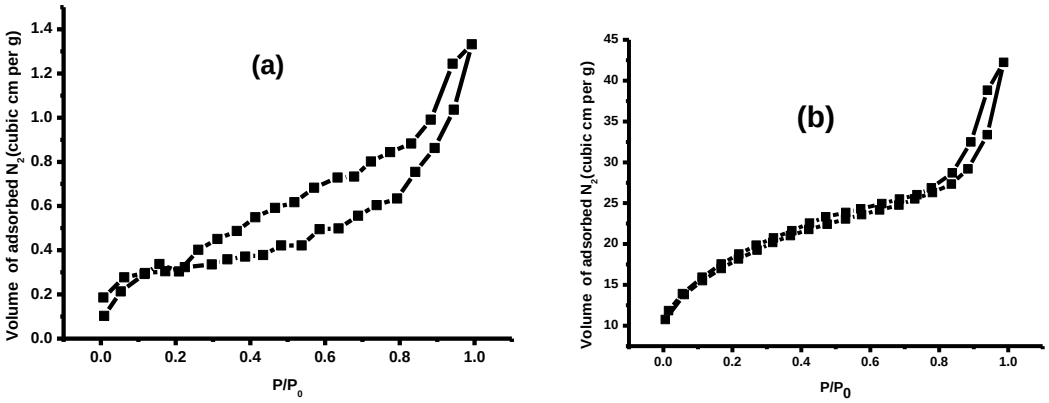

Fig. 14 Structural analyses of (a) SWCNHs and (b) water soluble SWCNHs

Total pore volume is 2.543e-01 cc/g for pristine SWCNHs with pores smaller than 1299.0 Å (Radius) at P/Po = 0.99257 where as in case of water soluble SWCNHs the total pore volume is 1.061e+00 cc/g with pores smaller than 756.5 Å (Radius) at P/Po = 0.98715. As for as average pore size is concerned it is higher for SWCNHs as compared to water soluble SWCNHs. Analyzed pore radius is 2.09068e+01 Å for water soluble SWCNHs and 9.15136e+02 Å for pristine SWCNHs. Since the water soluble SWCNHs have largely maintained its structure, the surface area of water soluble SWCNHs could be much higher than that of pristine SWCNHs.

A recorded room temperature PL spectrum for SWCNHs in fig 15 is tunable with excitation wavelengths.

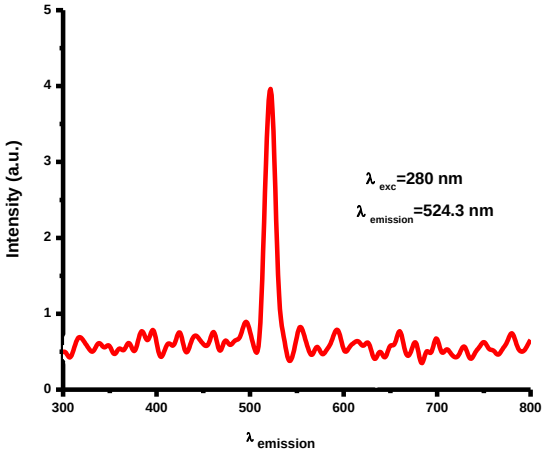

Fig. 15. PL spectra of SWCNHs

When the samples are exposed to high intensity radiations, the electrons are raised from the valence band to the excited states, and then these excited electrons return back to valence band with the emission of characteristic luminescent radiations. The intensity 'I' of the luminescent radiation at any time, t, is given by following equation

$$I = I_0 e^{-pt} \tag{2}$$

where I_0 is the intensity of radiation at cut-off position and the constant $p=1/\tau$ is the transition probability of the corresponding radiative transition. Here, τ is excited state lifetime, i.e. the time spent by electron in the trapping state before recombination. From the slope of the ln (I) vs. t, one

can easily calculate transition probability. Fig 16 show time resolved decay curves recorded for (a) SWCNHs and (b) water soluble SWCNHs.(WS-SWCNHs)

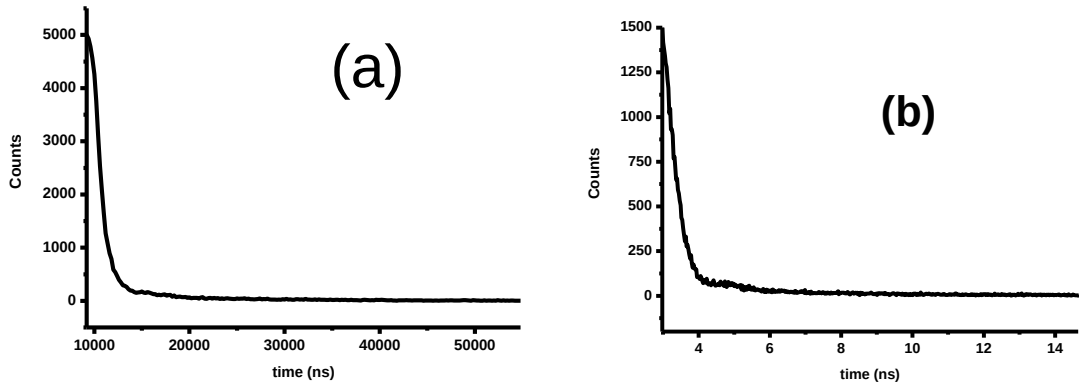

Fig. 16 (a) Time resolved decay curve for SWCNHs and (b) water soluble SWCNHs at room temperature

The Ln(I) vs. t graphs were plotted for all recorded decay curves. These Ln (I) vs. t graphs did not show linear relationship because of the superposition of a number of exponential decays. These graphs were peeled-off into maximum of three components using peeling-off method of Singh *et.al.* [25]. The slope of each component gives the value of transition probability (p) and hence the excited state lifetime 'τ'. Trap-depth values 'E' had been calculated using Boltzmann equation. All these values are listed in Tab 1

$$p = Se^{-E/kT} \tag{3}$$

where p is transition probability; S, escape frequency factor $\left(\sim 10^{9}\ s^{-1}\right)$; k, Boltzmann's constant and T, the absolute temperature.. Distribution of traps within the phosphor bandgap can be explained with the help of decay constant values. The decay constant value 'b' has been calculated using the equation

$$I = I_o t^{-b} \tag{4}$$

Such types of decay curves due to superposition of number of exponential decays are popularly known as hyperbolic decay curves or multi-exponential decay curves. If the value of, b, is unity, one can say that the distribution of trapping states is uniform, otherwise, it is said to be non-uniform. The Ln(I) vs. Ln(t) graph was plotted corresponding to emission wavelength; 525 nm for SWCNHs and WS-SWCNHs and decay constant 'b' value has been calculated from the slope of these graphs according to Equation. (4).For SWCNHs and WS-SWCNHs this value comes out to be more than one which means distribution of traps within the sample is uniform. In terms of lifetime values so calculated, one can calculate the oscillator strengths and dipole moments of the radiative transitions using well known equations. Electromagnetic radiation interacts with an electronic centre through the electric or magnetic field of the radiation. The oscillator strength 'f' of a transition is a dimensionless quantity that is useful for comparing different radiative transitions. Classically, oscillator strength is used as a statistical weight indicating the relative number of oscillators bound at each resonant frequency. In quantum mechanics, oscillator strength is used as a measure of relative strength of the electronic transitions within atomic and molecular systems. Oscillator strength is particularly useful as a technique for comparing transition "strengths" between different types of quantum mechanical systems. The life time values may also be used to calculate Einstein's spontaneous (A), stimulated emission (B) coefficients and dipole moment μ of the radiative transtion. Moreover the oscillator strength along with absorption coefficients is often used as a method for calculating the concentration of

impurities in a host. The oscillator strength of electric dipole allowed transitions [26-30] is given by the following relation

$$f_{ed}(\nu) = 1.5\times10^{4}.\lambda^{2}\frac{9}{\left(n^{2}+2\right)^{2}n}.p \tag{5}$$

where λ is the emission wavelength, p is the transition probability of the corresponding radiative transition and 'n' is the index of refraction of the material which is 1.586 in case of SWCNHs. The spontaneous radiative life-time is seen to be related in a simple way to the integrated cross section of the transition [26-30] by the following relation

$$I_{cs} = \frac{\lambda^{2}}{8\pi}.p \tag{6}$$

The corresponding dipole-moment [26-30] is given by the relation

$$\left|\mu\right| = \left(\frac{3h\varepsilon_{o}\lambda^{3}}{16\pi^{3}n}.p\right)^{\frac{1}{2}} \tag{7}$$

Dipole-moment values of SWCNHs were calculated by using equation (7) in terms of emission wavelength, index of refraction and the excited state life-time values.

Einstein's stimulated coefficient is given by following relation

$$B = \frac{2\pi^{2}\mu^{2}}{3n^{2}\varepsilon_{O}h^{2}} \tag{8}$$

where 'μ' is the dipole moment of transitions from the shallow trapping states of SWCNHs'ε_0' is the absolute permittivity of free space, 'n' is the index of refraction and 'h'is Planck's constant

Table 1. Transition Probability, Excited state life time and trap depth and other optical parameters of pristine and water soluble SWCNHs

	$p_{1\,(ns^{-1})}$	$p_{2\,(ns^{-1})}$	$p_{3(ns^{-1})}$
SWCNHs	$7.70269X10^{-4}$	$6.56664X10^{-4}$	$8.72137X10^{-5}$
WS-SWCNHs	2.54076	0.65586	0.25321
	τ_1(ns)	τ_2(ns)	τ_3(ns)
SWCNHs	1298.24	1522.84	11466.08
WS-SWCNHs	0.3935	1.5247	3.9492
	E_1(eV)	E_2(eV)	E_3(eV)
SWCNHs	0.3113	0.3131	0.3356
WS-SWCNHs	0.2209	0.2360	0.2466
	$I_{c1}(10^{-10}m^2s^1)$	$I_{c2}(10^{-10}m^2s^1)$	$I_{c3}(10^{-10}m^2s^1)$
SWCNHs	84.47	72.014	9.565
WS-SWCNHs	278639.31	71926.65	27768.95

	μ_1 ($X10^{-31}$Cm)	$\mu_{2\backslash}$ ($X10^{-31}$Cm)	μ_3 ($X10^{-31}$Cm)
SWCNHs	157.79	145.78	53.09
WS-SWCNHs	9045.35	4595.67	2855.51
	$f_1(X10^{-5})$	$f_2(X10^{-5})$	$f_3(X10^{-5})$
SWCNHs	88.652	75.577	10.0376
WS-SWCNHs	292422.18	75484.50	29142.54
	$B_1(X10^{18}m^3(rad/s)/Js)$	$B_2(X10^{18}m^3(rad/s)/Js)$	$B_3(X10^{18}m^3(rad/s)/Js)$
SWCNHs	167.91	143.33	19.009
WS-SWCNHs	547663.58	141371.14	54579.61

From the table 1 it is evident that average excited state life time for SWCNHs is 4762.38 ns where as for WS-SWCNHs the same is 1.9558 ns.

4. Conclusions

In summary, SWCNHs have been synthesized by submerged arc method and then functionalized with carboxylic and hydroxyl groups to make them water soluble which constitutes an efficient way for the chemical modification and solubilization of these materials. The method is complementary to other existing functionalization routes. Because the nanohorns are not deaggregated during the reaction and the round shaped aggregates remain intact in solution, the water dispersible. SWCNHs may be used in biotechnological applications, such as drug and gene delivery systems, as well as loading of the SWCNHs side-walls with desirable functional groups for specific tissue-targeting. Functionalization in SWCNHs has been confirmed by FTIR, Raman spectroscopy, Thermogravometric analysis and X ray photoelectron spectroscopy. Optical properties of SWCNHs has been analysed through energy resolved and time resolved PL. Further lifetime values calculated from decay curve have been used for the calculation of other important optical parameters of optoelectronic industrial interest like trap-depths, transition probabilities, oscillator strengths, Einstein's coefficients, integrated cross-sections, etc., which will be beneficial for optical calibration curves and detailed phosphor characterization for twenty-first century industrial applications. In brief this method of synthesis and functionalization is best method because high purity SWCNHs have been obtained through this method and the same has been confirmed through energy dispersive X ray spectroscopy. Structural property evaluated using BET-BJH technique reveals that functionalized SWCNHs have higher surface area and larger pore size as compared to pristine SWCNHs

Acknowledgements

Authors are thankful to Mr. Narender Budhiraja, Assistant Professor, G.H.G. Khalsa College, Gurusar Sadhar, Ludhiana for providing necessary facilities to bring this work in present form.

References

[1] S. Iijima, M Yudasaka, R Yamada, S Bandow, K Suenaga, F Kokai, K Takahashi Chem. Phys. Lett. **309**(3), 165 (1999).

[2] S. Bandow, F Kokai, K Takahashi, M Yudasaka, LC Qin and S Iijima Chem. Phys. Lett. **321**(5–6), 514 (2000)

[3] P J F Harris, S. C. Tsang, J. B. Claridge and M. L. H. Green J Chem Soc, Faraday Trans **90,** 2799 (1994)
[4] H. Kroto, J. R. Heath, S. C. O'Brien, R. F. Curl, R. E. Smalley Nature **318,** 162 (1995)
[5] S. Iijima, T. Ichihashi Nature **363,** 603 (1993)
[6] M. Yodasaka, S. Iijima, V.H. Crespi Topics Appl. Physics. **111**, 605 (2008)
[7] G**.** Pagona, G. Mountrichas, G. Rotas et al Int. J. Nanotechnology. **6**, 176 (2009).
[8] SY Zhu and GB Xu Nanoscale **2**(12), 2538 (2010)
[9] D Kasuya, M. Yudasaka, K. Takahashi, F Kokai and S Iijima J. Phys. Chem. B **106**(19), 4947 (2002)
[10] K Ajima, M Yudasaka,T. Murakami ,A Maigné ,K Shiba and S Iijima Mol. Pharm **2**(6), 475 (2005)
[11] K. Murata, A. Hashimoto, M. Yudasaka, D Kasuya and S Iijima. Adv.Mater. **16**(17), 1520 (2004).
[12] T. Yoshitakea, Y. Shimakawaa, S. Kuroshimaa, H. Kimuraa ,K Takahashic, F Kokaic, M Yudasakab, S Iijima Physica B **323,** 124 (2002)
[13] T Yamaguchi;S Bandow, S Iijima Chem. Phys. Lett. **389,** 181 (2004)
[14] G Pagona, A S D Sandanayaka ,Y Araki, J Fan, N Tagmatarchis, M Yuda, S Iijima, O. Ito, J. Phys. Chem. B **110** (42), 20729 (2006)
[15] G Pagona, ASD Sandanayaka , A Maigne, J Fan, G C Papavassiliou, I D Petsalakis , B R Steele, M Yudasaka, S Iijima, N Tagmatarchis and O Ito Chem. Eur. J. **13**(27), 7600 (2007)
[16] M Zhang, M Yudasaka ,K Ajima, J Miyawaki and S Iijima ACS Nano **1**(4), 265 (2007)
[17] C Cioffi, S Campidelli ,C Sooambar, M Marcaccio, G Marcolongo, M Meneghetti, D Paolucci, F Paolucci, C Ehli, G M A Rahman, V Sgobba, D M Guldi and M Prato J. Am. Chem. Soc. **129**(13), 3938 (2007)
[18] ASD Sandanayaka, O Ito, MF Zhang, K Ajima, S Iijima, M Yudasaka, T Murakami, K.Tsuchida Adv. Mater. **21**(43), 4366 (2009)
[19] M Vizuete, M J Gomez-Escalonilla ,JLG Fierro, ASD Sandanayaka, T Hasobe, M Yudasaka, S Iijima, O Ito and F Langa Chem. Eur. J. **16**(35), 10752 (2010)
[20] T Itoh, K Urita , E Bekyarova , M Arai, M Yudasaka, S Iijima, T Ohba, K Kaneko, H Kanoh J. Col. Interface Sci. **322,** 209 (2008)
[21] G Mountrichas, T Ichihashi ,S Pispas, M Yudasaka, S Iijima and N Tagmatarchis J. Phys. Chem. C **113**(14), 5444 (2009)
[22] W Huang, J Zhang, H C Dorn, D Geohegan and C Zhang Bioconjugate Chem. **22**(6), 1012 (2011)
[23] S Utsumi, H Honda, Y Hattori, H Kanoh, K Takahashi, H Sakai, M Abe, M Yudasaka, S Iijima, K J Kaneko, Phys.Chem. C **111**, 5572, (2007)
[24] E Miyako, H Nagata, K Hirano, Y Makita, K I Nakayama and T Hirotsu, Nanotechnology **18**, 475103 (1-7), (2007)
[25] K Singh, N K Verma, H S Bhatti Physica B **404,** 300 (2009)
[26] X L Wu, G G Siu, C L Fu, C H Ong, Appl.phys. Lett., **78**, 2285 (2001)
[27] D Kumar, K Singh, V Verma, H S Bhatti Adv. Sci. Eng. Med. **6** (2014) http://dx.doi.org/10.1166/asem.2014.1625
[28] D Kumar, K Singh, V Verma, H S Bhatti J. Bionanosci. **8** (2014) http://dx.doi.org/10.1166/jbns.2014.1236
[29] D Kumar, K Singh, V Verma, H S Bhatti J. Nanoelectron. Optoelectron **9** 458 (2014)
[30] D Kumar, Kavita, K Singh, V Verma, H S Bhatti Appl Nanosci (2014) http://link.springer.com/article/10.1007/s13204-014-0386-2